Robotica (2000) volume 18, pp. 381–387. Printed in the United Kingdom © 2000 Cambridge University Press

A new dynamic manipulability ellipsoid for redundant manipulators

Pasquale Chiacchio

Dipartimento di Informatica e Sistemistica, Università degli Studi di Napoli Federico II, Via Claudio 21, 80125 Napoli (Italy)
E-mail: pasquale.chiacchio@unina.it

(Received in Final Form: September 10, 1999)

SUMMARY
Manipulability ellipsoids are effective tools to perform task space analysis of robotic manipulators in terms of velocities, accelerations and forces at the end effector. In this paper a new definition of a dynamic manipulability ellipsoid for redundant manipulators is proposed which leads to more correct results in evaluating manipulator capabilities in terms of task-space accelerations. The case of manipulators in singular configurations is also analyzed. Two case studies are presented to illustrate the correctness of the proposed approach.

KEYWORDS: Robotics; Performance evaluation; Redundant manipulators

1. INTRODUCTION

Manipulability ellipsoids are effective tools for performing task space analyses of robotic manipulators, in terms of their ability to influence velocities and accelerations at the end effector or to exert forces on the environment. Briefly, they provide an approximate description of the maximum available performance of a manipulator in a given posture. This may be advantageous both in the design phase to determine the best manipulator's structure and size, and in the operational phase to find the best configuration to execute a given task.

The first definition of manipulability ellipsoids was given in reference 1 where the velocity manipulability ellipsoid was defined as the set of end-effector velocities which can be performed by joint velocities belonging to a unit sphere. By resorting to the duality principle, the force manipulability ellipsoid was also defined by giving an index of the ability of exerting end-effector forces along each task-space direction for a given set of joint torques. It can be shown that the principle axes of the two ellipsoids coincide, whereas the lengths of the axes are in inverse proportion; this property has been investigated in reference 2 to define suitable task compatibility indices.

In all those cases where the manipulator dynamics cannot be neglected, it is useful to consider the dynamic manipulability ellipsoid[3] which gives a measure of the ability to perform end-effector accelerations in a given posture with the joint torques constrained to belong to a unit sphere. A more correct formulation of the dynamic manipulability ellipsoid was given in reference 4 where the effects of the gravity are correctly taken into account.

Despite their popularity, ellipsoids suffer from possible inconsistency deriving from the improper use of the Euclidean metric and from the dependency on the change of scale and coordinate frame.[5] To overcome these problems, it is supposed here that all the joints are of the same kind (rotational) and that the relevant task space is composed of either linear or angular accelerations.

Alternative means to evaluate manipulator performance are task-space polytopes which accurately represent the maximum achievable task space capabilities with given limits in the joint space. In reference 6 a formal definition of force and velocity polytopes was given and the extension to two cooperating manipulators was discussed. In reference 7 the acceleration radius was derived from the acceleration polytope to characterize dynamic performances. In reference 8 the derivation of velocity polytope for redundant parallel robot was investigated. The definitions of manipulability ellipsoids given in references 1–4 are also extended to the case of redundant manipulators by using the unweighted pseudoinverse of the Jacobian matrix, but this is not always correct. It[9] has been demonstrated that a new definition of the force manipulability ellipsoid is necessary for redundant manipulators in order to satisfy the static assumption.

In our paper a new definition of dynamic manipulability ellipsoid for redundant manipulators is proposed which leads to more correct results in evaluating manipulator capabilities in terms of task-space accelerations. The case of manipulators in singular configuration is also analyzed. The paper is organized as follows: In Section 2 the basic relations are presented and the concepts of dynamic manipulability polytope and ellipsoid are introduced. Section 3 deals with the definition of the dynamic manipulability ellipsoid for nonredundant manipulator in nonsingular configuration. The extension to the case of redundant manipulators is questioned and a new definition of the dynamic manipulability ellipsoid for redundant manipulators is proposed in Section 4. The case of singular configurations is analyzed in Section 5. Two case studies are presented in Section 6 to illustrate the correctness of the proposed approach.

2. BASIC RELATIONS

Consider a general manipulator with n degrees of freedom whose end effector acts in an m-dimensional task space,

$m \leqslant n$. The first and second-order differential kinematics of the manipulator can be written as

$$\dot{\boldsymbol{x}} = \boldsymbol{J}(\boldsymbol{q})\dot{\boldsymbol{q}} \tag{1}$$

and

$$\ddot{\boldsymbol{x}} = \boldsymbol{J}(\boldsymbol{q})\ddot{\boldsymbol{q}} + \dot{\boldsymbol{J}}(\boldsymbol{q})\dot{\boldsymbol{q}}, \tag{2}$$

where $\boldsymbol{q} \in \mathcal{R}^n$ and $\boldsymbol{x} \in \mathcal{R}^m$ denote the joint and task variables, respectively, and $\boldsymbol{J} \in \mathcal{R}^{m \times n}$ is the Jacobian matrix. The manipulator's dynamics can be written as

$$\tau - \boldsymbol{J}(\boldsymbol{q})^{\mathrm{T}}\boldsymbol{h} = \boldsymbol{B}(\boldsymbol{q})\ddot{\boldsymbol{q}} + \boldsymbol{c}(\boldsymbol{q}, \dot{\boldsymbol{q}}) + \boldsymbol{g}(\boldsymbol{q}), \tag{3}$$

where $\boldsymbol{\tau} \in \mathcal{R}^n$ is the vector of joint torques, $\boldsymbol{h} \in \mathcal{R}^m$ is the vector of end-effector forces, $\boldsymbol{B} \in \mathcal{R}^{n \times n}$ is the symmetric, positive-definite inertia matrix, $\boldsymbol{c} \in \mathcal{R}^n$ is the vector of Coriolis and centrifugal torques, and $\boldsymbol{g} \in \mathcal{R}^n$ is the vector of gravitational torques. Hereafter, the dependence on $\boldsymbol{q}$ will be omitted for notational compactness.

The goal is to study the dynamic manipulability of the manipulator in terms of the mapping between joint torques and end-effector accelerations. It is considered that the manipulator is stationary in a given configuration $\bar{\boldsymbol{q}}$ and the end effector is not constrained (*i.e.*, $\boldsymbol{q} = \bar{\boldsymbol{q}}$, $\dot{\boldsymbol{q}} = \boldsymbol{0}$, $\boldsymbol{h} = \boldsymbol{0}$).

Under the above assumption, the second-order differential kinematic equation (2) simplifies to

$$\ddot{\boldsymbol{x}} = \boldsymbol{J}\ddot{\boldsymbol{q}} \tag{4}$$

and the dynamics (3) becomes

$$\tau = \boldsymbol{B}\ddot{\boldsymbol{q}} + \boldsymbol{g}. \tag{5}$$

Solving (5) for $\ddot{\boldsymbol{q}}$ gives

$$\ddot{\boldsymbol{q}} = \boldsymbol{B}^{-1}(\tau - \boldsymbol{g}) \tag{6}$$

which plugged into (4) results into

$$\ddot{\boldsymbol{x}} = \boldsymbol{J}\boldsymbol{B}^{-1}\tau + \ddot{\boldsymbol{x}}_g, \tag{7}$$

where

$$\ddot{\boldsymbol{x}}_g = -\boldsymbol{J}\boldsymbol{B}^{-1}\boldsymbol{g}. \tag{8}$$

It can be seen from (7) that the end-effector acceleration vector $\ddot{\boldsymbol{x}}$ for a given configuration is obtained by the superposition of the contributions of the joint torque vector $\boldsymbol{\tau}$ and the gravitational torque vector $\boldsymbol{g}$. The set of achievable end-effector accelerations can be obtained by translating by the quantity $\ddot{\boldsymbol{x}}_g$ the set of accelerations described by the mapping $\boldsymbol{J}\boldsymbol{B}^{-1}\boldsymbol{\tau}$, when $\boldsymbol{\tau}$ spans the set of all allowed joint torques.

Bounds for joint torques are usually velocity dependent. Since the manipulator is supposed still, constant bounds are considered here. The bounds are also assumed to be symmetric. If they were not, a suitable transformation can be performed.

Therefore, the $2n$ bounding inequalities for the joint torques.

$$|\tau_i| \leq \tau_i^{max}, \qquad i = 1, \ldots, n \tag{9}$$

are defined.

In the general case where the bounds of each joint torque are not equal, it is useful to scale them and thus consider normalized joint torques, *i.e.*

$$\tilde{\boldsymbol{\tau}} = \boldsymbol{L}^{-1}\boldsymbol{\tau} \tag{10}$$

where $\boldsymbol{L} = \mathrm{diag}(\tau_1^{\max}, \ldots, \tau_n^{\max})$ is the scaling matrix. At this point, the inequalities (9) can be written in a compact form as

$$\|\tilde{\tau}\|_\infty \leq 1 \tag{11}$$

where $\|\tilde{\boldsymbol{\tau}}\|_\infty = \max\{|\tilde{\tau}_1|, \ldots, |\tilde{\tau}_n|\}$. Equation (11) defines a hypercube in the space of normalized joint torques.

Rewriting (6) and (7) in terms of the normalized joint torques results into

$$\ddot{\boldsymbol{q}} = \boldsymbol{B}^{-1}\boldsymbol{L}\tilde{\boldsymbol{\tau}} - \boldsymbol{B}^{-1}\boldsymbol{g} \tag{12}$$

and

$$\ddot{\boldsymbol{x}} = \boldsymbol{M}\tilde{\boldsymbol{\tau}} + \ddot{\boldsymbol{x}}_g, \tag{13}$$

where

$$\boldsymbol{M} = \boldsymbol{J}\boldsymbol{B}^{-1}\boldsymbol{L}. \tag{14}$$

It is worth noticing that $\boldsymbol{M} \in \mathcal{R}^{m \times n}$ has the same rank as $\boldsymbol{J}$, since $\boldsymbol{B}$ and $\boldsymbol{L}$ are positive-definite matrices.

To find all the possible end-effector accelerations, the linear relation (13) must be considered with the set of joint torques defined by (11). This defines a convex polytope $\mathcal{P}$ as

$$\mathcal{P} \equiv \{\ddot{\boldsymbol{x}} = \boldsymbol{M}\tilde{\boldsymbol{\tau}} + \ddot{\boldsymbol{x}}_g \quad \text{with} \quad \|\tilde{\boldsymbol{\tau}}\|_\infty \leq 1\}. \tag{15}$$

The polytope $\mathcal{P}$ in (15) exactly describes manipulator's performances in terms of achievable end-effector accelerations.

The dynamic manipulability ellipsoid, as introduced by Yoshikawa,[3] gives instead an approximation of the manipulator's capabilities; this is interesting since it can be computed more simply and it makes it possible to define manipulability measures (e.g. the ellipsoid's volume) which might be derived analytically. The dynamic manipulability ellipsoid $\mathcal{E}$ is defined as

$$\mathcal{E} \equiv \{\ddot{\boldsymbol{x}} = \boldsymbol{M}\tilde{\boldsymbol{\tau}} + \ddot{\boldsymbol{x}}_g \quad \text{with} \quad \|\tilde{\boldsymbol{\tau}}\| \leq 1\}. \tag{16}$$

The only difference with the polytope's definition (15) is the use of the Euclidean norm instead of the infinity norm, *i.e.* it is supposed that the joint torques belong to the unit sphere in the normalized joint torque space.

It is clear by the definitions that the ellipsoid $\mathcal{E}$ is contained into the polytope $\mathcal{P}$. The vector $\ddot{\boldsymbol{x}}_g$ denotes the position of the center of both the polytope and the ellipsoid. This center coincides with the origin of the task-space acceleration space only if there are no gravitational torques or these torques do not cause, in the given configuration, a motion of the end-effector (that is the vector $\boldsymbol{B}^{-1}\boldsymbol{g}$ belongs to the null space of the Jacobian matrix $\boldsymbol{J}$)[4].

3. NONREDUNDANT MANIPULATORS IN NONSINGULAR CONFIGURATIONS

If the manipulator is nonredundant and in a nonsingular configuration, the matrix $\boldsymbol{M}$ in (14) is square and full rank, and thus equation (13) can be solved to give

$$\tilde{\boldsymbol{\tau}} = \boldsymbol{M}^{-1}(\ddot{\boldsymbol{x}} - \ddot{\boldsymbol{x}}_g) \tag{17}$$

which allows an explicit expression for the dynamic manipulability ellipsoid to be derived. The unit sphere in the space of normalized joint torques

https://doi.org/10.1017/S0263574799002106 Published online by Cambridge University Press

$$\tilde{\boldsymbol{\tau}}^{\mathrm{T}}\tilde{\boldsymbol{\tau}} \leq 1 \tag{18}$$

maps onto the ellipsoid in the task space of end-effector accelerations

$$(\ddot{\boldsymbol{x}}-\ddot{\boldsymbol{x}}_g)^{\mathrm{T}}\boldsymbol{M}^{-\mathrm{T}}\boldsymbol{M}^{-1}(\ddot{\boldsymbol{x}}-\ddot{\boldsymbol{x}}_g) \leq 1 \tag{19}$$

which, by using the definition (14) of $\boldsymbol{M}$ and introducing the new matrix

$$\boldsymbol{Q}=(\boldsymbol{L}^{-1}\boldsymbol{B})^{\mathrm{T}}\boldsymbol{L}^{-1}\boldsymbol{B}=\boldsymbol{B}\boldsymbol{L}^{-2}\boldsymbol{B}, \tag{20}$$

can be written as

$$(\ddot{\boldsymbol{x}}+\boldsymbol{J}\boldsymbol{B}^{-1}\boldsymbol{g})^{\mathrm{T}}\boldsymbol{J}^{-\mathrm{T}}\boldsymbol{Q}\boldsymbol{J}^{-1}(\ddot{\boldsymbol{x}}+\boldsymbol{J}\boldsymbol{B}^{-1}\boldsymbol{g}) \leq 1 \tag{21}$$

Ellipsoid (21) has all its principal axes of non null length, since its core

$$\boldsymbol{N}=\boldsymbol{J}^{-\mathrm{T}}\boldsymbol{Q}\boldsymbol{J}^{-1} \tag{22}$$

is positive definite. Given a direction in the task space characterized by the unit vector $\boldsymbol{t}$, the end effector of the manipulator can be accelerated in that direction with the acceleration a satisfying the inequality

$$\alpha a^2+2\beta a+\gamma \leq 0 \tag{23}$$

which has been derived by substituting $\ddot{\boldsymbol{x}}=a\boldsymbol{t}$ in (21). The coefficients in (23) are $\alpha=\boldsymbol{t}^{\mathrm{T}}\boldsymbol{N}\boldsymbol{t}>0$, $\beta=-\boldsymbol{t}^{\mathrm{T}}\boldsymbol{N}\ddot{\boldsymbol{x}}_g$, and $\gamma=\ddot{\boldsymbol{x}}_g^{\mathrm{T}}\boldsymbol{N}\ddot{\boldsymbol{x}}_g-1$.

If $\beta^2-\alpha\gamma$ in (23) is not negative, all the accelerations a belonging to the interval

$$\left[\frac{-\beta-\sqrt{\beta^2-\alpha\gamma}}{\alpha}, \frac{-\beta+\sqrt{\beta^2-\alpha\gamma}}{\alpha}\right] \tag{24}$$

can be realized, otherwise there are no achievable accelerations in that direction. This could happen[4] if the gravitational torques move the ellipsoid far from the line intersecting the origin of the axes whose direction is given by $\boldsymbol{t}$.

It is worth noticing that, in the nonredundant case, the ellipsoid (21) can be derived by solving the second order differential kinematics (4) as

$$\ddot{\boldsymbol{q}}=\boldsymbol{J}^{-1}\ddot{\boldsymbol{x}} \tag{25}$$

substituting (25) in (5), computing $\tilde{\boldsymbol{\tau}}$ as in (10) and putting it in (18). This is the definition as given in reference 3.

4. REDUNDANT MANIPULATORS IN NONSINGULAR CONFIGURATIONS

In references 3 and 4 the extension of the dynamic manipulability ellipsoid (21) to redundant arms is proposed by resorting to the unweighted pseudoinverse of the Jacobian matrix $\boldsymbol{J}^{\dagger}=\boldsymbol{J}^{\mathrm{T}}(\boldsymbol{J}\boldsymbol{J}^{\mathrm{T}})^{-1}$. This leads to the solution for the second-order differential kinematics

$$\ddot{\boldsymbol{q}}=\boldsymbol{J}^{\dagger}\ddot{\boldsymbol{x}} \tag{26}$$

and in turns to the definition of the dynamic manipulability ellipsoid as

$$(\ddot{\boldsymbol{x}}+\boldsymbol{J}\boldsymbol{B}^{-1}\boldsymbol{g})^{\mathrm{T}}\boldsymbol{J}^{\dagger\mathrm{T}}\boldsymbol{Q}\boldsymbol{J}^{\dagger}(\ddot{\boldsymbol{x}}+\boldsymbol{J}\boldsymbol{B}^{-1}\boldsymbol{g}) \leq 1 \tag{27}$$

What is questioned here is that whether using the solution (26) for the second-order differential kinematics leads to a correct definition of the dynamic manipulability ellipsoid. Equation (26) gives only one possible solution to the inverse differential kinematics, the one that minimizes the Euclidean norm of $\ddot{\boldsymbol{q}}$. This does not guarantee that the corresponding dynamic manipulability ellipsoid is that which better characterizes the manipulator's performance in terms of end-effector accelerations.

Therefore, a different derivation of the dynamic manipulability ellipsoid is proposed here. If the manipulator is redundant and is in a nonsingular configuration, the matrix $\boldsymbol{M}$ in (14) has more columns than rows and it is full rank. This implies that a nonempty null space of $\boldsymbol{M}$, denoted by $\mathrm{Ker}(\boldsymbol{M})$, exists. In order to compute the ellipsoid, it is then possible to consider only the projection of the unit sphere in the normalized joint torque space onto the orthogonal space of the null space $\mathrm{Ker}^{\perp}(\boldsymbol{M})=\mathrm{Im}(\boldsymbol{M}^{\mathrm{T}})$. This ensures that the bound on the normalized torques (18) is fully exploited, since torques which do not correspond to end-effector accelerations are not considered.

Inverting equation (13) using the unweighted pseudoinverse of $\boldsymbol{M}$ leads to

$$\tilde{\boldsymbol{\tau}}=\boldsymbol{M}^{\dagger}(\ddot{\boldsymbol{x}}-\ddot{\boldsymbol{x}}_g) \tag{28}$$

which only gives $\tilde{\boldsymbol{\tau}} \in \mathrm{Im}(\boldsymbol{M}^{\mathrm{T}})$.

The unit sphere in the space of normalized joint torques (18) now maps onto the ellipsoid in the task space of end-effector accelerations.

$$(\ddot{\boldsymbol{x}}-\ddot{\boldsymbol{x}}_g)^{\mathrm{T}}\boldsymbol{M}^{\dagger\mathrm{T}}\boldsymbol{M}^{\dagger}(\ddot{\boldsymbol{x}}-\ddot{\boldsymbol{x}}_g) \leq 1 \tag{29}$$

By recalling definitions (14) of $\boldsymbol{M}$ and (20) of $\boldsymbol{Q}$, an alternative expression is

$$(\ddot{\boldsymbol{x}}+\boldsymbol{J}\boldsymbol{B}^{-1}\boldsymbol{g})^{\mathrm{T}}(\boldsymbol{J}\boldsymbol{Q}^{-1}\boldsymbol{J}^{\mathrm{T}})^{-1}(\ddot{\boldsymbol{x}}+\boldsymbol{J}\boldsymbol{B}^{-1}\boldsymbol{g}) \leq 1 \tag{30}$$

Now, by introducing the weighted pseudoinverse of the Jacobian

$$\boldsymbol{J}_Q^{\dagger}=\boldsymbol{Q}^{-1}\boldsymbol{J}^{\mathrm{T}}(\boldsymbol{J}\boldsymbol{Q}^{-1}\boldsymbol{J}^{\mathrm{T}})^{-1} \tag{31}$$

equation (30) can be rewritten as

$$(\ddot{\boldsymbol{x}}+\boldsymbol{J}\boldsymbol{B}^{-1}\boldsymbol{g})^{\mathrm{T}}\boldsymbol{J}_Q^{\dagger\mathrm{T}}\boldsymbol{Q}\boldsymbol{J}_Q^{\dagger}(\ddot{\boldsymbol{x}}+\boldsymbol{J}\boldsymbol{B}^{-1}\boldsymbol{g}) \leq 1 \tag{32}$$

which can be directly compared with (27). To find achievable accelerations in the task space, equation (23) can still be used with $\boldsymbol{N}=\boldsymbol{J}_Q^{\dagger\mathrm{T}}\boldsymbol{Q}\boldsymbol{J}_Q^{\dagger}$.

It is interesting to evaluate the solution of the second-order differential kinematics which leads to the new definition (32) of the dynamic manipulability ellipsoid in the case of redundantt manipulators. From (12) and (28) it can be derived that

$$\ddot{\boldsymbol{q}}=\boldsymbol{J}_Q^{\dagger}\ddot{\boldsymbol{x}}-(\boldsymbol{I}-\boldsymbol{J}_Q^{\dagger}\boldsymbol{J})\boldsymbol{B}^{-1}\boldsymbol{g} \tag{33}$$

The inverse differential kinematics (33) gives the relation between all the end-effector accelerations belonging to the ellipsoid $\boldsymbol{\mathcal{E}}$ and the admissible joint accelerations (*i.e.* those for which $\tilde{\boldsymbol{\tau}}^{\mathrm{T}}\tilde{\boldsymbol{\tau}} \leq 1$) which could produce them. By construction, equation (33) is the solution to the problem

$$\min_{\ddot{q}}(\|\boldsymbol{L}^{-1}(\boldsymbol{B}\ddot{\boldsymbol{q}}+\boldsymbol{g})\|) \quad \text{with} \quad \boldsymbol{J}\ddot{\boldsymbol{q}}=\ddot{\boldsymbol{x}} \tag{34}$$

The first term on the right-hand side of (33) is the solution of (4) which minimizes the norm $\ddot{\boldsymbol{q}}^{\mathrm{T}}\boldsymbol{Q}\ddot{\boldsymbol{q}}$, while the second term is the projection of the vector $-\boldsymbol{B}^{-1}\boldsymbol{g}$ in the null space of $\boldsymbol{J}$. By analyzing the structure of matrix $\boldsymbol{Q}$ in (20) it can be concluded that solution (33) penalizes the joints which have a larger inertia-to-maximum-torque ratio. This is particularly evident when matrix $\boldsymbol{B}$ is diagonal, since matrix $\boldsymbol{Q}$ is diagonal too with elements $Q_{ii}=(B_{ii}/\tau_i^{\max})^2$.

5. MANIPULATORS IN SINGULAR CONFIGURATIONS

If the manipulator, whatever redundant or not, is in a singular configuration, the matrix $\boldsymbol{M}$ is not full rank. A non empty null space exists also for non redundant manipulator and, as above, it is possible to consider only the projection of the unit sphere in the normalized joint torque space onto the orthogonal space of the null space. Also, not all the rows of $\boldsymbol{M}$ are necessary to generate the accelerations $\ddot{\boldsymbol{x}}-\ddot{\boldsymbol{x}}_g$ in (13).

The singular value decomposition of $\boldsymbol{M}$ is

$$\boldsymbol{M}=[\boldsymbol{U}_1\ \ \boldsymbol{U}_2]\begin{bmatrix}\boldsymbol{\Sigma} & \boldsymbol{0}\\ \boldsymbol{0} & \boldsymbol{0}\end{bmatrix}\begin{bmatrix}\boldsymbol{V}_1^{\mathrm{T}}\\ \boldsymbol{V}_2^{\mathrm{T}}\end{bmatrix} \tag{35}$$

where $\boldsymbol{U_1}\in R^{m\times r}$, $U_2\in R^{m\times(m-r)}$, $V_1\in R^{n\times r}$, $V_2\in R^{n\times(n-r)}$. It can be shown that the following properties hold:[10]

(i) columns of $\boldsymbol{U}_1$ are an orthonormal base for $\mathrm{Im}(\boldsymbol{M})$;
(ii) columns of $\boldsymbol{U}_2$ are an orthonormal base for $(\mathrm{Im}(\boldsymbol{M}))^{\perp}=\mathrm{Ker}(\boldsymbol{M}^{\mathrm{T}})$;
(iii) columns of $\boldsymbol{V}_1$ are an orthonormal base for $(\mathrm{Ker}(\boldsymbol{M}))^{\perp}=\mathrm{Im}(\boldsymbol{M}^{\mathrm{T}})$;
(iv) columns of $\boldsymbol{V}_2$ are an orthonormal base for $\mathrm{Ker}(\boldsymbol{M})$.

Inverting equation (13) gives

$$\tilde{\boldsymbol{\tau}}=\boldsymbol{M}^{\#}(\ddot{\boldsymbol{x}}-\ddot{\boldsymbol{x}}_g) \tag{36}$$

where $\boldsymbol{M}^{\#}$ denotes the generalized inverse of $\boldsymbol{M}$ whose expression is

$$\boldsymbol{M}^{\#}=\boldsymbol{V}_1\boldsymbol{\Sigma}^{-1}\boldsymbol{U}_1^{\mathrm{T}}. \tag{37}$$

Equation (36) is the minimum (Euclidean) norm solution of (13).

Substituting (36) into (18), the expression of the dynamic manipulability ellipsoid in this case can be shown to be

$$(\ddot{\boldsymbol{x}}+\boldsymbol{J}\boldsymbol{B}^{-1}\boldsymbol{g})^{\mathrm{T}}\boldsymbol{U}_1\boldsymbol{\Sigma}^{-2}\boldsymbol{U}_1^{\mathrm{T}}(\ddot{\boldsymbol{x}}+\boldsymbol{J}\boldsymbol{B}^{-1}\boldsymbol{g})\le 1. \tag{38}$$

The ellipsoid in the m-dimensional space has $m-r$ principal axes of null length which denote directions where it is not possible for the manipulator to accelerate. These directions are those belonging to $\mathrm{Im}^{\perp}(\boldsymbol{M})$, the space generated by the columns of $\boldsymbol{U}_2$. To find achievable accelerations in the other directions, equation (23) may be used with $\boldsymbol{N}=\boldsymbol{U}_1\Sigma^{-2}\boldsymbol{U}_1^T$.

To evaluate the solution of the second-order differential equation which leads to the definition (38), from (12), (20) and (36) it can be derived that

$$\ddot{\boldsymbol{q}}=\boldsymbol{Q}^{-\frac{1}{2}}(\boldsymbol{J}\boldsymbol{Q}^{-\frac{1}{2}})^{\#}(\ddot{\boldsymbol{x}}-\ddot{\boldsymbol{x}}_g)-\boldsymbol{B}^{-1}\boldsymbol{g}. \tag{39}$$

Equation (39) can be written as

$$\ddot{\boldsymbol{q}}=\boldsymbol{J}_Q^{\#}\ddot{\boldsymbol{x}}-(\boldsymbol{I}-\boldsymbol{J}_Q^{\#}\boldsymbol{J})\boldsymbol{B}^{-1}\boldsymbol{g}. \tag{40}$$

by defining the generalized weighted inverse of $\boldsymbol{J}$

$$\boldsymbol{J}_Q^{\#}=\boldsymbol{Q}^{-\frac{1}{2}}(\boldsymbol{J}\boldsymbol{Q}^{-\frac{1}{2}})^{\#} \tag{41}$$

The name given to (41) is justified by the fact that $\ddot{\boldsymbol{q}}=\boldsymbol{J}_Q^{\#}\ddot{\boldsymbol{x}}$ is the solution of the problem

$$\min_{\ddot{q}}(\ddot{\boldsymbol{q}}^{\mathrm{T}}\boldsymbol{Q}\ddot{\boldsymbol{q}})\quad \text{with}\quad \boldsymbol{J}\ddot{\boldsymbol{q}}=\ddot{\boldsymbol{x}}. \tag{42}$$

By using (41), the ellipsoid (38) can be written in the alternative form

$$(\ddot{\boldsymbol{x}}+\boldsymbol{J}\boldsymbol{B}^{-1}\boldsymbol{g})^{\mathrm{T}}\boldsymbol{J}_Q^{\#\mathrm{T}}\boldsymbol{Q}\boldsymbol{J}_Q^{\#}(\ddot{\boldsymbol{x}}+\boldsymbol{J}\boldsymbol{B}^{-1}\boldsymbol{g})\le 1 \tag{43}$$

which can be compared with (27) and (32).

6. CASE STUDIES

To show the correctness of the proposed definition, we applied it to a three degree-of-freedom planar manipulator moving in the vertical plane, so that gravity forces act downward. The dynamic parameters of the manipulator's links in SI units are reported in the table below where l_i is the length, l_{ci} is the distance of the center of mass from the joint axes, and m_i is the mass of the i-th link.

Link	l_i	l_{ci}	m_i
1	1.0	0.5	4.0
2	0.8	0.4	2.0
3	0.5	0.25	0.6

The link inertia has been set as $I_i=m_i l_i^2/3$, $i=1, 2, 3$. The bounds on the joint torques are

$$\boldsymbol{\tau}_{\max}=-\boldsymbol{\tau}_{\min}=\begin{bmatrix}100\\30\\4\end{bmatrix}.$$

The manipulator has been set in the configuration

$$\boldsymbol{q}=\begin{bmatrix}\frac{\pi}{2}\\ -\frac{\pi}{2}\\ -\frac{\pi}{2}\end{bmatrix}.$$

The core of ellipsoid (27) is

$$\boldsymbol{N}=\begin{bmatrix}1.8011 & -0.9571\\ -0.9571 & 2.1908\end{bmatrix}10^{-3}$$

which gives the two eigenvectors

$$\begin{bmatrix}0.7744 & 0.6326\\ 0.6326 & -0.7744\end{bmatrix}$$

with the corresponding eigenvalues 18.341 and 31.323, respectively.

The core of ellipsoid (32) is

$$\boldsymbol{N}=\begin{bmatrix}0.5349 & 0.1752\\ 0.1752 & 1.1784\end{bmatrix}10^{-3}$$

https://doi.org/10.1017/S0263574799002106 Published online by Cambridge University Press

which gives the two eigenvectors

$$\begin{bmatrix} 0.9691 \\ -0.2467 \end{bmatrix} \quad \begin{bmatrix} 0.2467 \\ 0.9691 \end{bmatrix}$$

with the corresponding eigenvalues 28.595 and 45.163, respectively.

The vector $\ddot{\boldsymbol{x}}_g$ in (8) is $[0 \quad -12.392]^T$.

In Figure 1 the two dynamic manipulability ellipsoids (27) and (32) are plotted together with the polytope (15). Notice the difference between the two ellipsoids both in size and in orientation. Comparison with the polytope, which represents the exact mapping, confirms that the new definition of the dynamic manipulability ellipsoid presented in this paper gives better information about manipulator capabilities, as anticipated in the derivation of (32).

Consider now the horizontal direction in the task space denoted by $\boldsymbol{t}=[1 \quad 0]^{\mathrm{T}}$. By solving inequality (23) for the new definition of the ellipsoid (that is with $\boldsymbol{N}=\boldsymbol{J}_Q^{\dagger\mathrm{T}}\boldsymbol{Q}\boldsymbol{J}_Q^{\dagger}$) the achievable end-effector accelerations (24) are $a \in [-43.401, 35.284]$.

With reference to acceleration $\ddot{\boldsymbol{x}}=[35.284 \quad 0]^T$, by applying (33) the corresponding joint acceleration vector $\ddot{\boldsymbol{q}}=[6.8943 \quad -6.8943 \quad 84.356]^T$ is obtained which, substituting in $\tilde{\boldsymbol{\tau}}=\boldsymbol{L}^{-1}(\boldsymbol{B}\ddot{\boldsymbol{q}}+\boldsymbol{g})$, gives the needed normalized joint torque vector $\tilde{\boldsymbol{\tau}}=[0.3020 \quad 0.5247 \quad 0.7959]^T$. This torque is of unit norm and thus admissable.

If inversion (26) is applied instead, results are quite different. In fact, the resulting joint acceleration vector is now $\ddot{\boldsymbol{q}}=[-23.522 \quad 23.522 \quad 23.522]^T$ and the normalized joint torque vector is $\tilde{\boldsymbol{\tau}}=[-0.7879 \quad 0.5754 \quad 1.1761]^T$. This torque is not admissable since $\|\tilde{\boldsymbol{\tau}}\|=1.5281$; moreover the third component violates the real bounds on the normalized torque since it is greater than one.

Consider now the singular configuration

$$\boldsymbol{q} = \begin{matrix} \frac{\pi}{6} \\ 0 \\ 0 \end{matrix} .$$

which corresponds to a fully extended arm.

In this configuration, vector $\boldsymbol{x}_g$ in (8) is $[4.5579 \quad -7.8945]^T$. Matrix $\boldsymbol{M}$ in (14) is

$$\boldsymbol{M} = \begin{bmatrix} -5.4745 & 16.012 & -25.858 \\ 9.4820 & -27.735 & 44.787 \end{bmatrix}.$$

which has rank equal 1. Its Singular Value Decomposition is

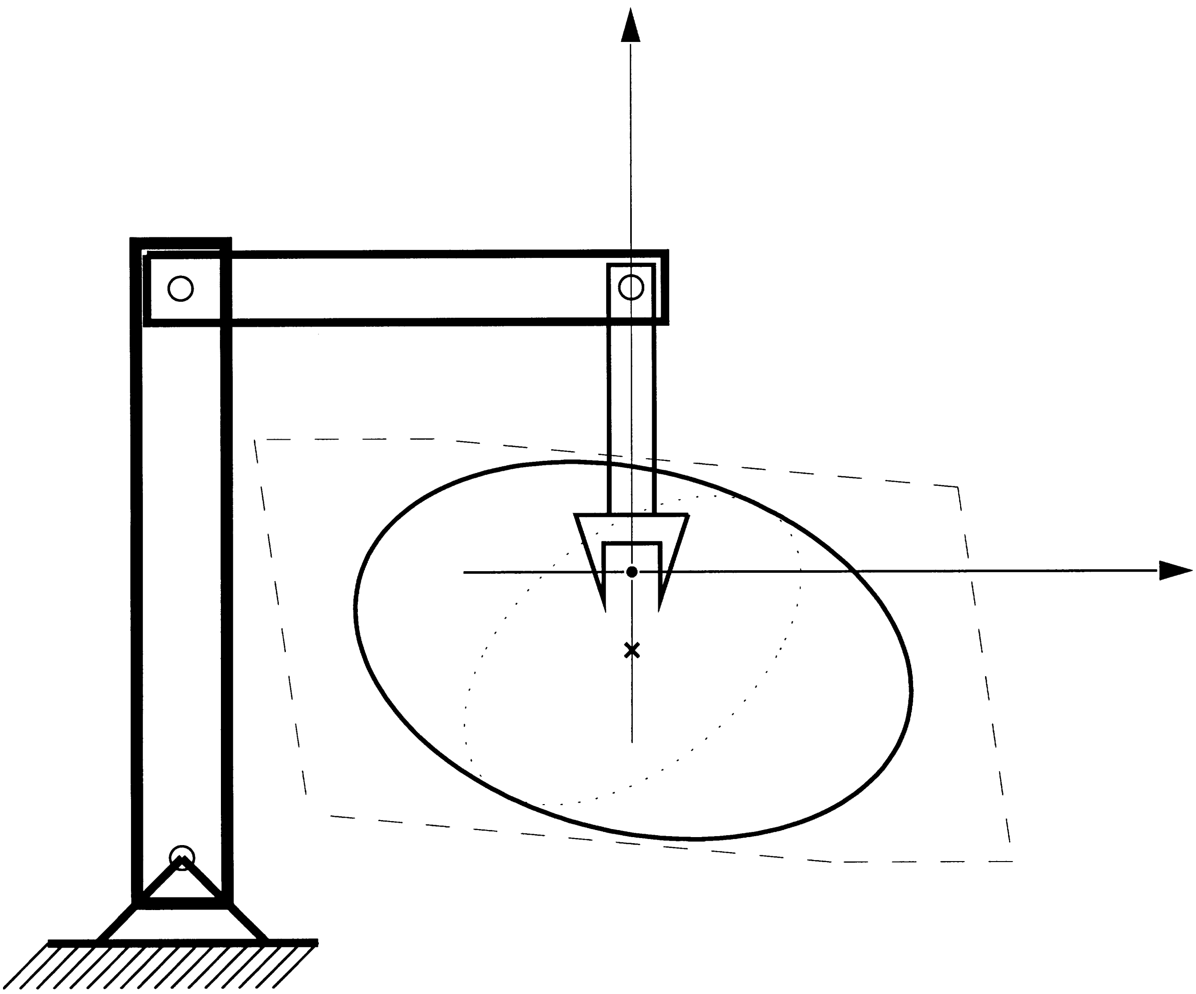

Fig. 1. The dynamic manipulator ellipsoids (27) –dotted– and (32) –solid-together with polytope (15) –dashed.

https://doi.org/10.1017/S0263574799002106 Published online by Cambridge University Press

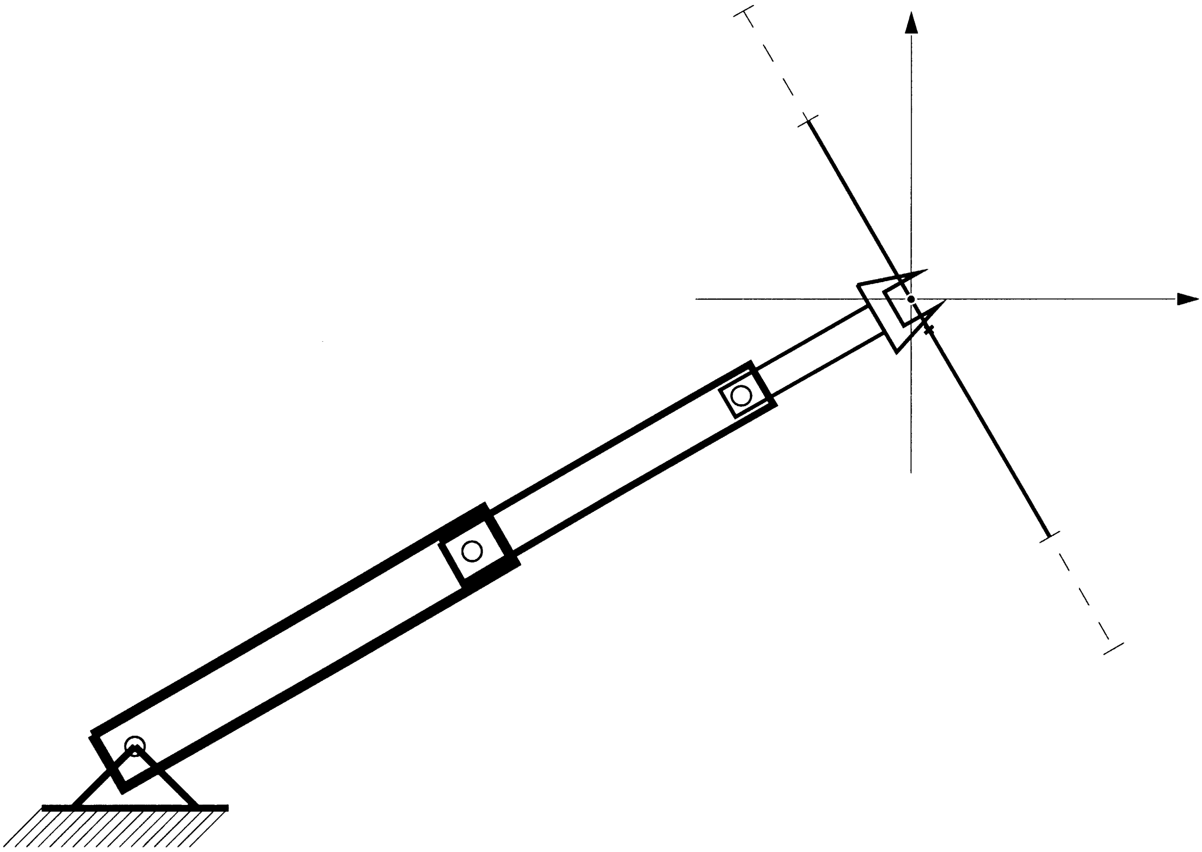

Fig. 2. The degenerated dynamic manipulability ellipsoids (38) –solid– together with polytope (15) –dashed.

$$\boldsymbol{M} = \begin{bmatrix} -0.5 & 0.866 \\ 0.866 & 0.5 \end{bmatrix} \begin{bmatrix} 61.806 & 0 & 0 \\ 0 & 0 & 0 \end{bmatrix}$$

$$\begin{bmatrix} 0.1771 & -0.5182 & 0.8367 \\ -0.9640 & 0.0798 & 0.2535 \\ 0.1982 & 0.8515 & 0.4854 \end{bmatrix}$$

The core of ellipsoid (38) is computed as $\boldsymbol{N} = \boldsymbol{U}_1 \boldsymbol{\Sigma}^{-2} \boldsymbol{U}_1^{\mathrm{T}}$ and it is

$$\boldsymbol{N} = 10^{-3} \begin{bmatrix} 0.0654 & -0.1134 \\ -0.1134 & 0.1963 \end{bmatrix}.$$

Notice that the ellipsoid degenerates into a segment. The end-effector's motions are only possible along the direction $\boldsymbol{U}_1 = [-0.5 \;\; 0.866]^T$, that is the direction orthogonal to the arm. Figure 2 shows the sought degenerate ellipsoid together with the polytope which also degerates into a segment.

The achievable end-effector's accelerations along that direction are those belonging to the interval (24) that in this case is $[-70.922, \; 52.690]$. With reference to the lower bound, consider the task-space acceleration $\ddot{\boldsymbol{x}} = [35.461 \; -61.420]^T$. By applying (40) the corresponding joint acceleration vector $\ddot{\boldsymbol{q}} = [-49.417 \;\; 172.961 \;\; -364.223]^T$ is obtained which gives the normalized joint torque $\tilde{\boldsymbol{\tau}} = [-0.1771 \; 0.5182 \;\; -0.8367]^T$.

This torque vector is of unit norm and thus admissible.

7. CONCLUSIONS

A new definition of the dynamic manipulability ellipsoid for redundant manipulators has been given in this paper. Differently from a previous definition, it more correctly characterizes a manipulator's performance in terms of achievable end-effector accelerations for a given set of joint torques. The case of manipulators in singular configurations has been also analyzed and a definition of dynamic manipulability ellipsoid given as well.

Two case studies for an "easy-to-understand" planar arm have been presented to show the correctness of the proposed definition.

ACKNOWLEDGMENTS

This work was supported jointly by *Ministero dell' Università e della Ricerca Scientifica e Technologica* and *Agenzia Spaziale Italiana*. Thanks to Ing. Mariano Concilio for helping devising the case studies.

References

1. T. Yoshikawa, "Manipulability of robotic mechanisms," *Robotics Research: The Second International Symposium* (H. Hanafusa and H. Inoue, eds.) (MIT Press, Cambridge, MA 1985) pp. 439–446.
2. S. Chiu, "Task compatibility of manipulator postures," *Int. J. Robotic Research* **7** (5) 13–21 (1988).
3. T. Yoshikawa, "Dynamic manipulability of robot manipulators," *J. Robotic Systems* **2** 113–124. (1985).
4. P. Chiacchio, S. Chiaverini, L. Sciavicco and B. Siciliano, "Influence of gravity on the manipulability ellipsoid for robot arms," *ASME Journal of Dynamic Systems, Measurement and Control* **114** 723–727. (1992).

5. K.L. Doty, C. Melchiorri, E.M. Schwartz and C. Bonivento, "Robot manipulability," *IEEE Transactions on robotics and automation* **11** 462–468 (1995).
6. T. Kokkinis and B. Paden, "Kinetostatic performance limits of coorperating robots using force-velocity polytopes," *Proceedings of the ASME Winter Annual Meeting-Robotics Research* San Francisco, CA (1989) pp. 151–156.
7. T.J. Graettinger and B.H. Krogh, "The acceleration radius: A global performance measure for robotic manipulators," *IEEE Journal of Robotics and Automation* **4** 60–69 (1988).
8. F. Pierrot and P. Chiacchio, "Evaluation of velocity capabilities for redundant parallel robots," *Proc. of the IEEE International Conference on Robotics and Automation* Albuquerque, NM (1997) pp. 774–779.
9. P. Chiacchio, Y. Bouffard-Vercelli and F. Pierrot, "Force polytope and force ellipsoid for redundant manipulators," *J. Robotic Systems* **14** 613–620 (1997).
10. V.C. Klema and A.J. Laub, "The singular value decomposition: Its computation and some applications," *IEEE Transactions an Automatic Control* **25**, 164–176 (1980).